ELSEVIER

Journal of Organometallic Chemistry 516 (1996) 1–10

Journal of Organometallic Chemistry

Coordination chemistry of organometallic polydentate ligands Studies on the syntheses and properties of Fe–M binuclear complexes prepared from organometallic tridentate ligand trans-$Fe(CO)_3(Ph_2Ppy)_2$ (Ph_2Ppy = 2-(diphenylphosphino)pyridine)

Zheng-Zhi Zhang [a,*], Hui Cheng [a], Shan-Ming Kuang [a], Yong-Qia Zhou [b], Zhi-Xian Liu [b], Jing-Kun Zhang [c], Hong-Gen Wang [c]

[a] *Elemento-Organic Chemistry Laboratory, Nankai University, Tianjin 300071, People's Republic of China*
[b] *Department of Chemistry, Nankai University, Tianjin 300071, People's Republic of China*
[c] *Central Laboratory, Nankai University, Tianjin 300071, People's Republic of China*

Received 27 April 1995; in revised form 6 December 1995

Abstract

The binuclear complexes $(CO)_3Fe(\mu\text{-}Ph_2Ppy)_2MX_n$ (Ph_2Ppy = 2-(diphenylphosphino)pyridine, MX_n = $Mn(SCN)_2$, $Co(SCN)_2$, $CoCl_2$, $NiCl_2$, $Mo(CO)_3$, $Zn(SCN)_2$, $ZnCl_2$, $Cd(SCN)_2$, $CdCl_2$, $HgCl_2$, HgI_2, $AgClO_4$, and $SnCl_2$) were prepared from the new type of organometallic tridentate ligand, *trans*-$Fe(CO)_3(Ph_2Ppy)_2$ (**1**), which contains both a basic metal center and bridging phosphine ligands. The crystal structure of the benzene solvate of **1** was determined by X-ray diffraction. The compound $\mathbf{1} \cdot 1/2C_6H_6$ crystallizes in the monoclinic space group $P2_1/c$ with a = 17.560(5), b = 12.110(1), c = 18.176(4) Å; β = 101.27(2)° and Z = 4. The structure was refined to a conventional R value of 0.077 by using 2670 significant reflections and parameters. The structure of one of the binuclear complexes, namely, $(CO)_3Fe(\mu\text{-}Ph_2Ppy)_2HgI_2$ (**14**), has also been determined by X-ray diffraction. The compound **14** crystallizes in the monoclinic space group $P2_1/n$, with a = 13.829(2), b = 14.175(2), c = 19.514(3) Å, β = 120.27(1)°, V = 3738(2) Å^3 and Z = 4. The structure was refined to a conventional R value of 0.032 by using 3279 significant reflections and parameters. The Fe–Hg distance is 2.678 Å, indicative of a metal–metal bond. Results of Mössbauer and electron-absorption spectra suggested the presence of metal to metal interactions in these binuclear complexes.

Keywords: Organometallic polydentate ligand; Donor–acceptor bond; Binuclear complex; Synthesis; Structure

1. Introduction

In the past decades, it has been found that a variety of homo-and heterobinuclear complexes can be synthesized by oxidative addition [1] or condensation [2] reaction in which 2-(diphenylphosphino)pyridine (Ph_2Ppy) acts as a bridging ligand.

Recently, we have paid considerable attention to the basicity of the metal, which arises from the potential of the basic metal to form a binuclear complex. The basicity of the metal has been studied for many years [3], but there are only limited utilities in forming binuclear complexes where the basic metal may act as a donor to donate electrons to another metal and a donor–acceptor bond may be formed. Some examples include $Fe(CO)_5 \cdot HgCl_2$ [4], $CpCo(CO)_2HgCl_2$ [5], $(OC)_5OsOs(CO)_3(GeCl_3)Cl$ [6], $(\eta^5\text{-}C_5Me_5)(OC)_2IrW(CO)_5$ [7], $(OC)_4(^tBuNC)OsCr(CO)_5$ [8], $(Me_3P)(OC)_4OsRe(CO)_4Br$ [9], $(OC)_4CoRh(CO)(PEt_3)_2$ [10], and $(OC)_5OsM(CO)_5$ (M = Cr, W) [11], etc. For the binuclear complexes $(OC)_5OsM(CO)_5$ (M = Cr, W), the nature of the dative metal–metal bonds has been investigated by ab initio molecular orbital calculation [11]. In contrast, little attention has been paid to the common effects of basic metals and phosphine bridging ligands on the formation of binuclear complexes, though phosphine bridging ligands offer the opportunity to synthesize binuclear complexes.

* Corresponding author.

PII S0022-328X(96)06118-9

A previous paper [1m] from our laboratory has described that the organometallic tridentate ligand, *trans*-$Fe(CO)_3(Ph_2Ppy)_2$ (**1**), can directly coordinate to a second metal atom through the two pyridine nitrogens and the basic iron center. This provided a new approach for synthesis of Ph_2Ppy bridging binuclear complexes.

In this article, we report our further investigation on the X-ray structure and the reactivity of organometallic tridentate ligand, *trans*-$Fe(CO)_3(Ph_2Ppy)_2$ (**1**), and on the preparation and characterization of some binuclear complexes $(CO)_3Fe(\mu\text{-}Ph_2Ppy)_2MX_n$ (MX_n = $Mn(SCN)_2$, $Co(SCN)_2$, $CoCl_2$, $NiCl_2$, $Mo(CO)_3$, $Zn(SCN)_2$, $ZnCl_2$, $Cd(SCN)_2$, $CdCl_2$, $HgCl_2$, HgI_2, $AgClO_4$, and $SnCl_2$). The metal–metal interaction in these binuclear complexes has been investigated by Mössbauer and electron-absorption spectroscopies and, in the case of $(CO)_3Fe(\mu\text{-}Ph_2Ppy)_2HgI_2$ (**14**), has been confirmed by an X-ray diffraction study.

2. Results and discussion

2.1. Synthesis and characterization of the binuclear complexes

A recent quantitative study on the linear correlations between the basicity of metal and phosphine ligands in *trans*-$Fe(CO)_3(PR_3)_2$ has revealed that *trans*-$Fe(CO)_3(PPh_3)_2$ is weakly basic [12]. However, no reaction has been reported between *trans*-$Fe(CO)_3(PPh_3)_2$ and metal compounds except HgX_2 (X = Cl, I) [4]. In contrast with that, compound **1** can react with many metal compounds to give homo- or heterobinuclear complexes by using both its basic metal center and bridging phosphine ligands, although Ph_2Ppy has a similar basicity to Ph_3P.

It is noteworthy that the analogous $HgCl_2$ and HgI_2 react differently with compound **1**. For $HgCl_2$, yellow crystals of $(CO)_3Fe(\mu\text{-}Ph_2Ppy)_2 \cdot 2HgCl_2$ (**13**) are given. This product is a 1 : 1 electrolyte in nitrobenzene and could be formulated as $[(CO)_3Fe(\mu\text{-}Ph_2Ppy)_2\text{-}HgCl]^+[HgCl_3]^-$ [13]. For HgI_2, this reaction produces a yellow crystalline $(CO)_3Fe(\mu\text{-}Ph_2Ppy)_2HgI_2$ (**14**), which is identified as containing an Fe–Hg bond by X-ray diffraction.

Reactions of compound **1** in dichloromethane with a solid MX_n or a suitable solution of MX_n (MX_n = $Mn(SCN)_2$, $Co(SCN)_2$, $CoCl_2$, $NiCl_2$, $Mo(CO)_3(MeCN)_3$, $Zn(SCN)_2$, $ZnCl_2$, $Cd(SCN)_2$, $CdCl_2$, $AgClO_4$, and $SnCl_2$) give $(CO)_3Fe(\mu\text{-}Ph_2Ppy)_2MX_n$. (When MX_n is $Mo(CO)_3(MeCN)_3$, the compound $(CO)_3Fe(\mu\text{-}Ph_2Ppy)_2Mo(CO)_3$ (**10**) is formed.) These compounds are fully characterized by IR, ^{31}P NMR, FD-MS and elemental analyses.

The IR spectra of these complexes have shown that the carbonyl stretching vibrational band has split into three peaks and shifted to higher frequencies compared with the parent **1**. This is consistent with both a change in stereochemistry and decrease in electron density on the iron atom. During the formation of the FeM binuclear compound, the iron atom transfers some of its electrons to the second metal with a higher oxidation state. The withdrawal in electron density from the iron atom results in the increase of the carbonyl-to-iron σ-donation and the decrease of the iron-to-carbonyl π-back donation. Both these effects cause the strengthening in C–O bond. In contrast, the split of carbonyl bands is associated with the change in the local symmetry of carbonyls on the iron atom from D_{3h} to C_{2v}.

The ^{31}P NMR spectra of these compounds in chloroform-*d* solution consist of a singlet which indicates that the two phosphorus atoms in these compounds remain chemically equivalent in comparison with compound **1**. For FeCd complex (**8**), or FeHg complexes (**13**) and (**14**), the couplings to Cd or Hg produce satellites to the main peak and two bond P–Fe–Cd or P–Fe–Hg couplings are observed. The magnitudes of the ^2J(Cd–P)(34 Hz) or ^2J(Hg–P) ($(CO)_3Fe(\mu\text{-}Ph_2Ppy)_2 \cdot 2HgCl_2$, 219 Hz; $(CO)_3Fe(\mu\text{-}Ph_2Ppy)_2HgI_2$, 190 Hz) are comparable with those of some compounds containing an Fe–M bond (M = Cd, Hg); for example, $(OC)_3Fe[Si(OMe)_3](\mu\text{-}Ph_2Ppy)Cd(4\text{-pic})Br$ (^2J(Cd–P), 82 Hz) [2g], $Cd[Fe(CO)_3\{Si(OMe)_3\}(\mu Ph_2Ppy)]_2$ (^2J(Cd–P), 66 Hz) [2g], $Hg[Fe(CO)_3(SiMePh_2)(PMe_3)]_2$ (^2J(Hg–P), 240.3 Hz) [14], $Hg[Fe(CO)_3(SiMePh_2)(PBu_3)]_2$ (^2J(Hg–P), 205.0 Hz) [14], and $Hg[Fe(CO)_3\{Si(OMe)_3\}(dppm\text{-}P)]_2$ (^2J(Hg–P), 173 Hz) [15], etc.

In the FD-MS spectra of these compounds, the presence of the $(M^+–X)$ peak indicates the formation of the expected binuclear complexes $(CO)_3Fe(\mu\text{-}Ph_2Ppy)_2\text{-}MX_n$.

2.2. Studies on metal–metal interactions

2.2.1. Mössbauer spectra

Mössbauer spectra of these binuclear complexes were obtained at 78 K. The observed Mössbauer parameters are listed in Table 1. All the isomer shifts fall into the range from -0.04 to -0.09 mm s^{-1}, and the quadruple splittings range from 1.34 to 2.11 mm s^{-1}. Compared with compound **1** (IS = -0.10 mm s^{-1}, QS = 2.59 mm s^{-1}), all the IS values are increased, while the QS values are decreased.

For the iron complexes, the isomer shift reflects the total electron density at the iron nucleus. It decreases either with increasing s-electron density through phosphorus-to-iron σ-donation or with decrease in the shielding of the s-electron by decreasing 3d-electron density through iron-to-phosphorus π-back donation. When a Ph_2Ppy bridging binuclear complex is formed, the nitrogen atom of the pyridinic ring would transfer its electrons to the second metal, and the phosphorus-to-iron

Table 1
Mössbauer parameter of $(CO)_3Fe(\mu\text{-}Ph_2Ppy)_2MX_n$

No	Complex	IS (mm s^{-1})	QS (mm s^{-1})
1	*trans*-$Fe(CO)_3(Ph_2Ppy)_2$	−0.10	2.59
2	$(CO)_3Fe(\mu\text{-}Ph_2Ppy)_2Zn(SCN)_2$	−0.06	1.82
3	$(CO)_3Fe(\mu\text{-}Ph_2Ppy)_2Cd(SCN)_2$	−0.04	1.83
4	$(CO)_3Fe(\mu\text{-}Ph_2Ppy)_2Co(SCN)_2$	−0.07	1.89
5	$(CO)_3Fe(\mu\text{-}Ph_2Ppy)_2Mn(SCN)_2$	−0.06	2.03
8	$(CO)_3Fe(\mu\text{-}Ph_2Ppy)_2CdCl_2$	−0.06	1.94
9	$(CO)_3Fe(\mu\text{-}Ph_2Ppy)_2ZnCl_2$	−0.09	1.93
10	$(CO)_3Fe(\mu\text{-}Ph_2Ppy)_2Mo(CO)_3$	−0.07	2.11
13	$(CO)_3Fe(\mu\text{-}Ph_2Ppy)_2 2HgCl_2$	−0.04	1.34

σ-donation would decrease due to the decrease of s-electron density at phosphorus. At the same time, the transfer of the 3d-electron from iron to the second metal would decrease the iron-to-phosphorus π-back donation, which would result in the increase in the shielding of the s-electron at the iron atom. Both these effects are consistent with the result of the increases in IS values for these binuclear complexes in comparison with compound **1**, indicative of the presence of an interaction between these two metal atoms. In contrary, the quadruple splitting is affected mainly by the electric field gradient around the iron nucleus and the asymmetry of the 3d-electrons which decreased with the increase of molecular symmetry and increasing electron-acceptor capability of the second metal atom. When a binuclear complex is formed, the 3d-electron configuration of the iron atom transforms from the trigonal bipyramid to an octahedron. This is in agreement with the decreasing QS values. At the same time, the Fe–M binuclear complex with a stronger Fe–M interaction would give a smaller quadruple splitting.

2.2.2. *Electron-absorption spectra*

Interestingly, we found that metal to metal charge transfer (MMCT) could be treated by Jørgensen's theory of charge transfer transitions. This provides evidence for the metal–metal interactions in binuclear compounds.

The charge transfer transition energies may be expressed by the following equation [16]:

$$E(\mathrm{cm}^{-1}) = 30{,}000[X(D) - X(A)] + \Delta OE + \Delta SPE \quad (1)$$

$X(D)$ and $X(A)$ are the optical electronegativities of the donor and the acceptor orbitals. ΔOE stands for the energy difference between the beginning or ending transition orbital and the orbital where optical electronegativity is defined as zero. ΔSPE is the correction of spin pairing energy, resulting from the change in d configuration during transition, and is represented by D, namely as a spin pairing energy parameter. Approximately, D is equal to $7B$, where B is the Racah parameter with an approximate value of 1000 cm^{-1}. In contrast, Dq is nearly equal to 1000 cm^{-1}.

The electron-absorption spectra are measured in a N_2 atmosphere with reference to dichloromethane solvent or the dichloromethane solution of compound **1**. Table 2 gives the observed results, and the assignments of MMCT and LMCT bands are listed in Table 3. Then we

Table 2
Electronic transition energies (cm^{-1}) of $(CO)_3Fe(\mu\text{-}Ph_2Ppy)_2MX_n$

MX_n	Reference to the solution of **1** in dichloromethane				Reference to the solvent of dichloromethane			
$Zn(SCN)_2$	37600	43100			38500	43300		
	(15600)	(4450)			(30000)	(39000)		
$Cd(SCN)_2$	36700	43100			37800	43700		
	(16800)	(5100)			(46000)	(66000)		
$HgCl_2$	41900	34300			34800	43300		
	(4320)	(126400)			(21000)	(46340)		
$Mn(SCN)_2$	23000	31500	36900		38700	43800		
	(110)	(120)	(790)					
$Co(SCN)_2$	21300	26400	37800	43200	21200	26600	38600	43500
	(960)	(5640)	(14600)	(8600)	(1060)	(6240)	(42800)	(67000)
$NiCl_2$	24500	31100	37800	43000	25000	31300	39200	43200
	(1820)	(640)	(12900)	(10000)	(2080)	(sh)	(36000)	(49000)
$Fe(CO)_3(PPh_3)_2 \cdot 2HgCl_2$		34200				43700	34700	
					(57000)	(23600)		

Data in parentheses stand for the molar absorbance.

Table 3
Assignments of LMCT and MMCT bands

Complex	LMCT (cm^{-1}) N–M (II, III)	MMCT (cm^{-1}) Fe(0)–M(II, III)
$(CO)_3Fe(\mu\text{-}Ph_2Ppy)_2Zn(SCN)_2$	43100	37600
$(CO)_3Fe(\mu\text{-}Ph_2Ppy)_2Cd(SCN)_2$	43100	36700
$(CO)_3Fe(\mu\text{-}Ph_2Ppy)_2 \cdot 2HgCl_2$	41900	34300
$(CO)_3Fe(\mu\text{-}Ph_2Ppy)_2Mn(SCN)_2$	31500	23000
$(CO)_3Fe(\mu\text{-}Ph_2Ppy)_2Co(SCN)_2$	26400	21300
$(CO)_3Fe(\mu\text{-}Ph_2Ppy)_2NiCl_2$	31100	24500
$(CO)_3Fe(Ph_3P)_2 \cdot 2HgCl_2$		34200

identified these assignments by comparing the X(M) values calculated by an improved Jørgensen's method with the literature ones.

For the FeM binuclear complexes formed, MMCT occurs from iron atom to the second metal atom, M, while LMCT occurs between the pyridine nitrogen atom and M. For M = Mn, Co, or Ni, the ΔOE and ΔSPE values in the LMCT transition are easily determined by the d^n configurations of various metal ions (Eq. (2)) [17]. However, considering the change of Fe(0) from d^8 to d^7 during the MMCT transitions, $-1/3D$ should be added to the ΔSPE term (Eq. (3)). This is a modification to Jørgensen's treatment while it is extended to deal with MMCT transitions. For M = Zn, Cd, Hg, the ΔOE and ΔSPE values need no correction. Thus, using Eqs. (2a) or (3a) together with the reported X(M(II)) [18] (M = Zn, Cd, and Hg), X(Fe(0)) and X(N) could be calculated. Then X(M) of the other metal ions could be obtained by Eqs. (2b)–(2d) and (3b)–(3d). These observed X(M) values agree well with the corresponding literature values (Table 4), indicating successful assignments of MMCT and LMCT bands.

N–Zn, Cd, Hg(II):

$$E(cm^{-1}) = 30000[X(L) - X(M)] \quad (2a)$$

N–Mn(II): $E(cm^{-1})$

$$= 30000[X(L) - X(M)] + 2/3D \quad (2b)$$

N–Co(II): $E(cm^{-1})$

$$= 30000[X(L) - X(M)] + 1.72Dq + 1/3D \quad (2c)$$

N–Ni(II): $E(cm^{-1})$

$$= 30000[X(L) - X(M)] + 10Dq - 4/3D \quad (2d)$$

Fe(0)–Zn, Cd, Hg(II): $E(cm^{-1})$

$$= 30000[X(Fe) - X(M)] - 1/3D \quad (3a)$$

Fe(0)–Mn(II): $E(cm^{-1})$

$$= 30000[X(Fe) - X(M)] + 1.72Dq + 1/3D \quad (3b)$$

Fe(0)–Co(II): $E(cm^{-1})$

$$= 30000[X(Fe) - X(M)] + 1.72Dq \quad (3c)$$

Fe(0)–Ni(II): $E(cm^{-1})$

$$= 30000[X(Fe) - X(M)] + 10Dq - 5/3D \quad (3d)$$

2.3. Crystal structure of $Fe(CO)_3(Ph_2Ppy)_2 \cdot 1/2C_6H_6$ (1)

The geometry of the $Fe(CO)_3(Ph_2Ppy)_2 \cdot 1/2C_6H_6$ (**1**) molecule and associated atomic numbering scheme are presented in Fig. 1. Table 5 gives final atomic coordinates and thermal factors of the non-hydrogen atoms. Some selected bond distances and angles are listed in Table 6.

Table 4
Comparison of calculated X(M) with literature values

M	X(M) calculated from LMCT	X(M) calculated from MMCT	Literature values
Zn(II)	1.47	—	1.48–1.51 (tetrahedron) [18]
Cd(II)	1.47	—	
Hg(II)	1.51	—	
Zn(II)	—	1.27	1.27–1.29 (linear) [18]
Cd(II)	—	1.30	
Hg(II)	—	1.38	
Mn(II)	2.01	1.97	—
Co(II)	2.16	1.95	1.8–1.9 (tetrahedron) [19]
Ni(II)	1.90	1.73	2.0–2.1 (tetrahedron) [19a] 2.2 (square plane) [19a]
Fe(0)		2.60	—

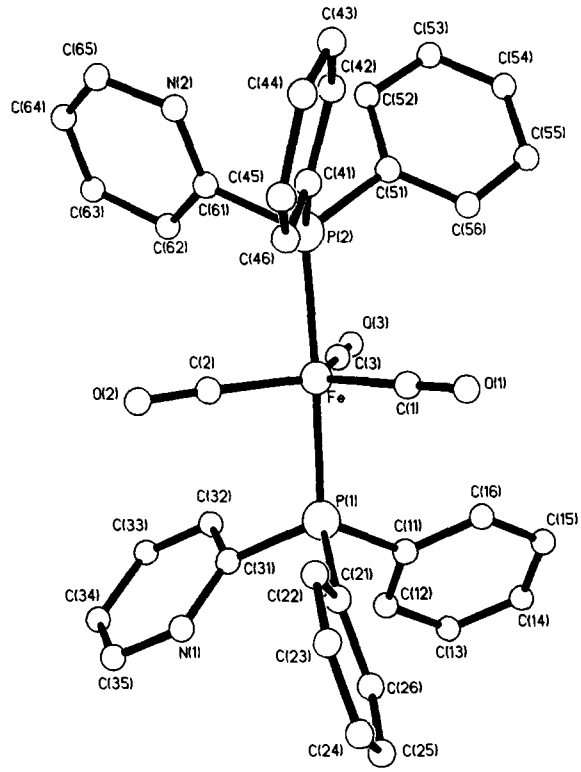

Fig. 1. View of molecule of $Fe(CO)_3(Ph_2Ppy)_2 \cdot 1/2C_6H_6$ (1).

The iron atom adopts an idealized trigonal bipyramidal configuration. The FeP_2 unit has the expected dimensions with Fe–P distances of 2.2022 Å and 2.2064 Å, and a P–Fe–P angle of 177.08°. The three carbonyl ligands occupy the three remaining coordination sites with an average C–O distance of 1.133 Å and an average Fe–C distance of 1.782 Å. The Fe–C–O units are nearly linear. Within the Fe–C(1)–C(2)–C(3) framework, the sum of all of the C–Fe–C angles is 359.9°, consistent with the fact that this unit is planar.

2.4. Crystal structure of $(CO)_3Fe(\mu\text{-}Ph_2Ppy)_2HgI_2$ (14)

A perspective drawing of this complex is shown in Fig. 2. Fractional coordinates and thermal parameters of non-hydrogen are given in Table 7. Table 8 contains selected interatomic distances and relevant bond angles.

For comparison with compound **1**, the trans P–Fe–P unit is also nearly linear with a P–Fe–P angle of 176.32°, while a compression of the angles between the carbonyl ligands at the iron center is observed due to the coordination of the mercury atom with the iron atom, and both C(2)–Fe–C(3) and C(1)–Fe–C(3) angles are below 110°. In contrast, the Fe–P and Fe–C distances are elongated by nearly 0.05 Å and 0.03 Å respectively. The iron atom exhibits an octahedral geometry.

The mercury atom is five-coordinate. In addition to the two iodine atoms, it is bonded to two pyridine nitrogen atoms and the iron atom. The two pyridine nitrogen atoms are trans to each other with the N(36)–Hg–N(66) angle of 168.5°. The Hg–N distances are 2.658 and 2.731 Å, which can be considered as weak

Table 5
Fractional coordinates and thermal parameters for non-hydrogen on $Fe(CO)_3(Ph_2Ppy)_2 \cdot 1/2C_6H_6$ (1)

Atom	x	y	z	B_{eq} (Å^2)
Fe	0.20907(6)	0.05703(8)	1.00056(6)	3.60(1)
P(1)	0.1826(1)	0.2311(1)	0.9710(1)	3.83(3)
P(2)	0.2408(1)	−0.1167(1)	1.0274(1)	3.51(3)
O(1)	0.0802(3)	0.0417(5)	1.0794(4)	5.9(1)
O(2)	0.3603(4)	0.1267(7)	1.0827(6)	7.5(2)
O(3)	0.1813(7)	−0.0022(7)	0.8416(4)	8.3(2)
C(1)	0.1293(4)	0.0478(6)	1.0478(5)	4.7(1)
C(2)	0.3019(4)	0.0979(6)	1.0496(5)	4.8(2)
C(3)	0.1923(5)	0.0215(8)	0.9032(6)	5.3(2)
C(11)	0.1000(4)	0.2540(6)	0.8936(5)	4.4(1)
C(12)	0.1070(6)	0.3308(6)	0.8449(5)	5.4(2)
C(13)	0.0116(8)	0.350(1)	0.7863(8)	7.5(3)
C(14)	−0.0248(6)	0.291(1)	0.7822(6)	6.6(2)
C(15)	−0.0311(7)	0.210(1)	0.8339(8)	7.5(3)
C(16)	0.0345(6)	0.1906(9)	0.8910(6)	5.9(2)
C(21)	0.1373(4)	0.3175(6)	1.0447(5)	4.4(1)
C(22)	0.1813(5)	0.2882(7)	1.1204(5)	5.1(2)
C(23)	0.1628(6)	0.3564(9)	1.1757(5)	5.9(2)
C(24)	0.1239(6)	0.4528(8)	1.1575(5)	5.7(2)
C(25)	0.1001(6)	0.4816(7)	1.0846(7)	6.0(2)
C(26)	0.1161(5)	0.4145(6)	1.0287(7)	5.7(2)
C(31)	0.2617(5)	0.3066(6)	0.9419(5)	4.8(2)
C(32)	0.2863(7)	0.268(1)	0.8809(9)	8.0(3)
C(33)	0.3462(9)	0.324(2)	0.851(1)	10.7(1)
C(34)	0.3782(6)	0.429(1)	0.893(1)	10.2(3)
C(35)	0.3526(6)	0.456(1)	0.954(2)	10.7(3)
N(1)	0.2930(5)	0.9989(9)	0.9785(9)	8.4(3)
C(41)	0.2129(1)	−0.1616(6)	1.1234(4)	3.8(1)
C(42)	0.2357(8)	−0.2727(8)	1.1392(5)	5.6(2)
C(43)	0.2408(7)	−0.307(1)	1.2125(7)	6.1(2)
C(44)	0.2554(8)	−0.233(1)	1.2703(5)	7.0(3)
C(45)	0.2593(8)	−0.120(1)	1.2535(6)	7.1(2)
C(46)	0.2524(5)	−0.0855(8)	1.1790(6)	5.5(2)
C(51)	0.1756(5)	−0.2195(6)	0.9716(4)	4.2(1)
C(52)	0.2056(4)	−0.3133(7)	0.9481(5)	4.5(1)
C(53)	0.1550(5)	−0.3865(7)	0.9049(5)	5.1(2)
C(54)	0.0791(5)	−0.3659(7)	0.8870(5)	5.2(2)
C(55)	0.0489(6)	−0.2729(7)	0.9124(7)	5.7(2)
C(56)	0.0986(4)	−0.1940(6)	0.9543(5)	4.6(1)
C(61)	0.3376(4)	−0.1553(6)	1.0141(5)	4.5(1)
C(62)	0.3708(6)	−0.103(1)	0.9631(7)	9.1(3)
C(63)	0.4480(7)	−0.135(2)	0.9538(8)	10.7(3)
C(64)	0.4821(6)	−0.215(1)	0.996(1)	8.6(4)
C(65)	0.4507(6)	−0.262(2)	1.046(1)	12.0(5)
N(2)	0.3747(7)	−0.237(1)	1.0542(9)	9.4(3)
C(71)	0.500(3)	0.506(5)	0.263(2)	14(1)
C(72)	0.432(1)	0.544(3)	0.235(1)	12.4(6)
C(73)	0.394(2)	0.477(3)	0.188(2)	11.3(8)
C(74)	0.417(2)	0.383(3)	0.170(1)	8.9(5)
C(75)	0.479(3)	0.340(3)	0.197(2)	10.2(8)
C(76)	0.522(2)	0.389(4)	0.255(3)	13(1)

Anisotropically refined atoms are given in the form of the equivalent isotropic thermal parameter defined as: $(4/3)[a^2\beta(1,1) + b^2\beta(2,2) + c^2\beta(3,3) + ab(\cos\gamma)\beta(1,2) + ac(\cos\beta)\beta(1,3) + bc(\cos\alpha)\beta(2,3)]$.

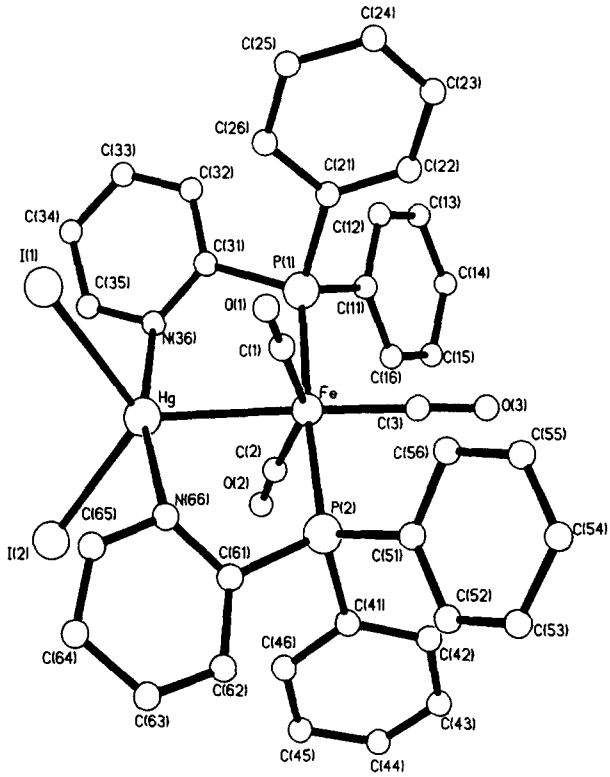

Fig. 2. View of molecule of $(CO)_3Fe(\mu\text{-}Ph_2Ppy)_2HgI_2$(**14**).

bonding interactions between the mercury and nitrogen atoms. The Fe–Hg separation of 2.678 Å falls in the long end of the range found for Fe–Hg complexes (Table 9), but is shorter than the sum of atomic radii, implying the presence of an Fe–Hg bond. Taking into account the weak bonding interactions of Hg–N, the coordination around mercury atom is elongated trigonal bipyramidal.

The three carbonyls, the iron atom and the mercury atom are also coplanar. The bridging Ph_2Ppy ligands are perpendicularly coordinated to that plane, and the bridging Ph_2Ppy ligands in a head-to-head arrangement on the two metal atoms show a significant skewing. This is reflected in the P–Fe–Hg–N torsional angles (22.91, 23.89°) and the shortening P · · · N distances (2.714 and 2.702 Å), in comparison with those found in compound **1** (2.794 and 2.730 Å).

3. Experimental section

Established methods were used to prepare the compounds Ph_2Ppy [1f], *trans*-$Fe(CO)_3(Ph_2Ppy)_2$ [1m] (**1**), $Mo(CO)_3(MeCN)_3$ [26]. Solvents were dried by standard procedures. All experiments were performed under an atmosphere of purified nitrogen. IR spectra were obtained by using a WFD-14 spectrometer. ^{31}P NMR spectra were recorded on an Fx-90Q spectrometer at 36.19 Hz. Phosphorus chemical shifts were referred to external 85% H_3PO_4 in $CDCl_3$. FD-MS spectra were measured on a Hitachi M-80. Conductivity measurements were made with a DDS-11A conductivity meter. Elemental analyses were carried out on a Perkin–Elmer model 240 analyzer.

Mössbauer effect spectra were made at 78 K on a constant-acceleration spectrometer, Model MS-500. Electron-absorption spectra were performed on a Schimadzu UV-260 in an atmosphere of nitrogen.

The reactions were generally monitored by IR in the γ(CO) region.

3.1. Synthesis of $(CO)_3Fe(\mu\text{-}Ph_2Ppy)_2M(SCN)_2$ (M = Zn, 2; Cd, 3; Co, 4)

A solution of **1** (0.4 g, 0.6 mmol) in 15 ml of dichloromethane was added to a solution of $M(SCN)_2$ (0.6 mmol) in 10 ml of methanol, and the resultant solution was stirred for 4–6 h at room temperature. During this time a color change occurred and a precipitate was formed. The solid was filtered, washed with diethyl ether and dried in vacuo. To the concentrated

Table 6
Selected bond distances (Å) and angles (deg) for $Fe(CO)_3(Ph_2Ppy)_2 \cdot 1/2C_6H_6$ (**1**)

Bond distances			
Fe–P(1)	2.2022(7)	Fe–C(1)	1.784(3)
Fe–P(2)	2.2064(7)	Fe–C(2)	1.769(3)
C(1)–O(1)	1.128(3)	Fe–C(3)	1.790(3)
C(2)–O(2)	1.138(4)	C(3)–O(3)	1.135(5)
Bond angles			
P(1)–Fe–P(2)	177.08(3)	P(2)–Fe–C(2)	89.26(8)
P(1)–Fe–C(1)	91.65(8)	P(2)–Fe–C(3)	88.6(2)
P(1)–Fe–C(2)	89.14(8)	C(1)–Fe–C(2)	120.5(1)
P(1)–Fe–C(3)	90.2(2)	C(1)–Fe–C(3)	117.9(1)
P(2)–Fe–C(1)	91.27(8)	C(2)–Fe–C(3)	121.5(1)
Fe–P(1)–C(11)	115.45(8)	Fe–P(2)–C(41)	116.99(9)
Fe–P(1)–C(21)	116.15(9)	Fe–P(2)–C(51)	114.61(8)
Fe–P(1)–C(31)	114.45(9)	Fe–P(2)–C(61)	114.63(8)
Fe–C(1)–O(1)	178.2(3)	Fe–C(2)–O(2)	177.5(3)
Fe–C(3)–O(3)	179.2(4)		

filtrates, diethyl ether was added to afford the further product.

3.1.1. $(CO)_3Fe(\mu\text{-}Ph_2Ppy)_2Zn(SCN)_2$ (2)

White solid. Yield: 0.35 g (68.9%). Anal. Found: C, 54.89; H, 3.42; N, 6.22. $C_{39}H_{28}FeN_4O_3P_2S_2Zn$. Calc.: C. 55.24; H, 3.33; N, 6.61%. IR: ν(CO), 2000w, 1965s, 1945s, cm^{-1}. FD-MS: *m / e* (relative intensity, %), 789 (M^+–SCN, 100), 787 (81).

Table 7
Fractional coordinates and thermal parameters for non-hydrogen on $(CO)_3Fe(\mu\text{-}Ph_2Ppy)_2HgI_2$ (14)

Atom	x	y	z	B (Å^2)
Hg	0.53474(2)	0.22813(3)	0.36801(2)	3.087(5)
I(1)	0.38452(5)	0.24051(6)	0.44295(3)	4.50(1)
I(2)	0.71835(5)	0.21127(8)	0.45404(4)	5.45(2)
Fe	0.49543(7)	0.23686(8)	0.22772(5)	2.35(2)
P(1)	0.4091(1)	0.1010(1)	0.2195(1)	2.59(4)
P(2)	0.5762(1)	0.3750(2)	0.2290(1)	2.68(4)
O(1)	0.3301(5)	0.3402(6)	0.2667(5)	4.8(2)
O(2)	0.6825(5)	0.1324(6)	0.2642(5)	4.7(2)
O(3)	0.4622(7)	0.2426(7)	0.0747(3)	5.1(2)
C(1)	0.3927(7)	0.2983(6)	0.2524(5)	3.6(2)
C(2)	0.6116(6)	0.1724(6)	0.2531(5)	3.1(2)
C(3)	0.4745(6)	0.2405(6)	0.1331(5)	3.3(2)
C(11)	0.4319(7)	0.0130(6)	0.1538(5)	3.2(2)
C(12)	0.3632(9)	−0.0572(8)	0.1323(7)	5.2(2)
C(13)	0.384(1)	−0.1238(8)	0.0877(9)	6.0(3)
C(14)	0.471(1)	−0.1220(7)	0.0629(6)	5.2(2)
C(15)	0.5410(8)	−0.0529(9)	0.0851(6)	4.9(2)
C(16)	0.5181(6)	0.0161(7)	0.1309(4)	3.4(2)
C(21)	0.2778(6)	0.1188(7)	0.1954(5)	3.1(2)
C(22)	0.2287(8)	0.1317(8)	0.1264(6)	4.5(2)
C(23)	0.127(1)	0.151(1)	0.108(1)	5.8(3)
C(24)	0.0740(9)	0.1544(9)	0.158(1)	6.3(3)
C(25)	0.1214(9)	0.145(1)	0.2295(8)	5.5(3)
C(26)	0.2217(8)	0.1313(9)	0.2485(7)	4.9(2)
C(31)	0.4246(6)	0.0233(6)	0.2984(4)	2.9(2)
C(32)	0.359(1)	−0.0427(8)	0.3058(7)	5.1(3)
C(33)	0.3719(9)	−0.0943(9)	0.3654(8)	5.7(3)
C(34)	0.451(1)	−0.081(1)	0.4165(7)	5.4(3)
C(35)	0.5148(9)	−0.0083(8)	0.4061(6)	4.6(2)
N(36)	0.5024(8)	0.0441(7)	0.3496(5)	4.2(2)
C(41)	0.6976(6)	0.3569(7)	0.2088(6)	4.4(2)
C(42)	0.7092(9)	0.354(1)	0.1391(6)	5.2(2)
C(43)	0.804(1)	0.340(2)	0.1291(6)	9.3(4)
C(44)	0.8784(9)	0.322(1)	0.181(1)	6.9(4)
C(45)	0.8715(8)	0.322(1)	0.2501(6)	6.2(2)
C(46)	0.7782(7)	0.337(1)	0.2628(9)	5.1(3)
C(51)	0.5166(7)	0.4638(6)	0.1651(4)	3.2(2)
C(52)	0.569(1)	0.540(1)	0.1470(9)	5.9(3)
C(53)	0.5239(9)	0.6074(8)	0.1025(9)	6.4(3)
C(54)	0.421(2)	0.6014(8)	0.0711(8)	6.6(3)
C(55)	0.371(1)	0.529(1)	0.0888(9)	6.2(3)
C(56)	0.4142(8)	0.4569(8)	0.1363(6)	4.7(2)
C(61)	0.6043(7)	0.4423(7)	0.3109(5)	3.2(2)
C(62)	0.6710(9)	0.517(1)	0.3233(8)	6.2(3)
C(63)	0.689(1)	0.558(1)	0.386(1)	7.6(3)
C(64)	0.638(1)	0.531(1)	0.4373(8)	6.2(3)
C(65)	0.573(1)	0.4641(8)	0.4194(8)	5.9(3)
N(66)	0.5517(6)	0.4194(7)	0.3589(4)	4.4(2)

Anisotropically refined atoms are given in the form of the isotropic equivalent displacement parameter defined as: $(4/3)[a^2\beta(1,1)+b^2\beta(2,2)+c^2\beta(3,3)+ab(\cos\gamma)\beta(1,2)+ac(\cos\beta)\beta(1,3)+bc(\cos\alpha)\beta(2,3)]$.

3.1.2. $(CO)_3Fe(\mu\text{-}Ph_2Ppy)_2Cd(SCN)_2$ (3)

White solid. Yield: 0.38 g (71%). Anal. Found: C, 52.60; H, 3.25; N, 5.97. $C_{39}H_{28}CdFeN_4O_3P_2S_2$. Calc.: C, 52.34; H, 3.15; N, 6.26%. IR: ν(CO), 2000w, 1965s, 1940s, cm^{-1}.

3.1.3. $(CO)_3Fe(\mu\text{-}Ph_2Ppy)_2Co(SCN)_2$ (4)

Pink solid. Yield: 0.32 g (64%). Anal. Found: C, 56.52; H, 3.35; N, 6.46. $C_{39}H_{28}CoFeN_4O_3P_2S_2$. Calc.: C, 55.65; H, 3.68; N, 6.66%. IR: ν(CO), 2000w, 1960s, 1937s, cm^{-1}.

3.2. Synthesis of $(CO)_3Fe(\mu\text{-}Ph_2Ppy)_2MX_2$ (MX_2 = $Mn(SCN)_2$, 5; $CoCl_2$, 6; $NiCl_2$, 7; $CdCl_2$, 8)

Solid MX_2 (0.6 mmol) was added to a well-stirred solution of **1** (0.4 g, 0.6 mmol) in dichloromethane (15 ml). The mixture was left under stirring for 4–6 h. The solid dissolved gradually to give a clear solution from which a precipitate was then formed. This was collected by filtration, washed with diethyl ether, and dried in vacuo. The product was purified by recrystallization from dichloromethane–hexane.

3.2.1. $(CO)_3Fe(\mu\text{-}Ph_2Ppy)_2Mn(SCN)_2$ (5)

Orange solid. Yield: 0.30 g (60%). Anal. Found: C, 55.84; H, 3.62; N, 6.44. $C_{39}H_{28}FeMnN_4O_3P_2S_2$. Calc.: C, 55.93; H, 3.37; N, 6.69%. IR: ν(CO), 1998w, 1953s, 1925s, cm^{-1}. FD-MS: *m / e* (relative intensity, %), 779 (M^+–SCN, 100), 780 (55).

3.2.2. $(CO)_3Fe(\mu\text{-}Ph_2Ppy)_2CoCl_2$ (6)

Yellowish-green solid. Yield: 0.26 g (55%). Anal. Found: C, 54.82; H, 3.41; N, 2.96. $C_{37}H_{28}Cl_2CoFeN_2O_3P_2$. Calc.: C, 55.78; H, 3.52; N, 3.52%. IR: ν(CO), 2000w, 1952s, 1930s, cm^{-1}.

3.2.3. $(CO)_3Fe(\mu\text{-}Ph_2Ppy)_2NiCl_2$ (7)

Pink solid. Yield: 0.31 g (55%). Anal. Found: C, 54.69; H, 3.56; N, 3.52. $C_{37}H_{28}Cl_2FeN_2NiO_3P_2$. Calc.: C, 55.78; H, 3.52; N, 3.52%. IR: ν(CO), 2000w, 1950s, 1930s, cm^{-1}. ^{31}P NMR: δ 80.36.

3.2.4. $(CO)_3Fe(\mu\text{-}Ph_2Ppy)_2CdCl_2$ (8)

White solid. Yield: 0.48 g (94.2%). Anal. Found: C, 51.72; H, 3.22; N, 2.92. $C_{37}H_{28}CdCl_2FeN_2O_3P_2$. Calc.: C, 52.27; H, 3.30; N, 3.30%. IR: ν(CO), 2000w, 1960s, 1942s, cm^{-1}. ^{31}P NMR: δ 80.36 (s, ^2J(Cd–P) = 34 Hz).

3.3. Synthesis of $(CO)_3Fe(\mu\text{-}Ph_2Ppy)_2ZnCl_2$ (9)

To a solution of **1** (0.4 g, 0.6 mmol) in dichloromethane (15 ml) was added a solution of $ZnCl_2$

Table 8
Selected bond distances (Å) and angles (deg) for $(CO)_3Fe(\mu\text{-}Ph_2Ppy)_2HgI_2$ (**14**)

Bond distances			
Fe–P(1)	2.2542(5)	Fe–C(1)	1.816(3)
Fe–P(2)	2.2511(6)	Fe–C(2)	1.823(2)
C(1)–O(1)	1.132(3)	Fe–C(3)	1.808(2)
C(2)–O(2)	1.113(3)	C(3)–O(3)	1.117(3)
Hg–I(1)	2.7886(1)	Hg–N(36)	2.658(2)
Hg–I(2)	2.7406(2)	Hg–N(66)	2.731(2)
Hg–Fe	2.6780(2)		
Bond angles			
P(1)–Fe–P(2)	176.32(9)	P(2)–Fe–C(2)	91.51(6)
P(1)–Fe–C(1)	89.78(6)	P(2)–Fe–C(3)	87.60(7)
P(1)–Fe–C(2)	90.81(6)	C(1)–Fe–C(2)	149.6(1)
P(1)–Fe–C(3)	89.08(7)	C(1)–Fe–C(3)	107.04(9)
P(2)–Fe–C(1)	89.66(6)	C(2)–Fe–C(3)	103.5(1)
Hg–Fe–P(1)	91.31(1)	Fe–P(1)–C(11)	117.15(7)
Hg–Fe–P(2)	92.08(2)	Fe–P(1)–C(21)	112.94(8)
Hg–Fe–C(1)	75.60(7)	Fe–P(1)–C(31)	118.61(7)
Hg–Fe–C(2)	73.97(6)	Fe–P(2)–C(41)	110.67(8)
Hg–Fe–C(3)	177.35(6)	Fe–P(2)–C(51)	115.99(7)
I(1)–Hg–I(2)	112.379(6)	Fe–P(2)–C(61)	103.1(2)
I(1)–Hg–N(36)	90.59(5)	Fe–C(1)–O(1)	177.0(2)
I(2)–Hg–N(36)	96.00(5)	Fe–C(2)–O(2)	175.6(2)
I(1)–Hg–N(66)	93.20(4)	Fe–C(3)–O(3)	179.6(2)
I(2)–Hg–N(66)	92.59(5)	Hg–C(2)–Fe	67.16(6)
I(1)–Hg–Fe	121.410(6)	Hg–C(2)–O(2)	117.3(2)
I(2)–Hg–Fe	126.195(7)	Hg–N(36)–C(31)	113.9(2)
Fe–Hg–N(36)	85.14(5)	Hg–N(36)–C(35)	117.0(2)
Fe–Hg–N(66)	83.64(5)	Hg–N(66)–C(61)	110.6(1)
N(36)–Hg–N(66)	168.51(7)	Hg–N(66)–C(65)	115.1(2)

(0.6 mmol) in diethyl ether and the reaction mixture was left stirring. After 2–4 h, a white precipitate was formed and collected by filtration, washed with diethyl ether and dried in vacuo. The white product was recrystallized from dichloromethane–hexane. Yield: 0.44 g (91.2%). Anal. Found: C, 55.02; H, 3.40; N, 3.03. $C_{37}H_{28}Cl_2FeN_2O_3P_2Zn$. Calc.: C, 55.36; H, 3.49; N, 3.49%. IR: ν(CO), 2000w, 1960s, 1940s, cm^{-1}. ^{31}P NMR: δ 80.77.

3.4. Synthesis of $(CO)_3Fe(\mu\text{-}Ph_2Ppy)_2Mo(CO)_3$ (10)

To an acetonitrile solution of fresh $Mo(CO)_3(MeCN)_3$ (0.6 mmol) was added a benzene solution (20 ml) of **1** (0.4 g, 0.6 mmol). Immediately, the color of the solution turned from orange to red-brown. After stirring for 0.5 h at room temperature, the volume of the solution was then reduced to 8 ml. By addition of diethyl ether (20 ml), a red-brown precipitate was obtained. This was filtered, washed with diethyl ether, and dried in vacuo to give the product in 70.9% yield. Anal. Found: C, 57.89; H, 3.30; N, 3.27. $C_{40}H_{28}FeMoN_2O_6P_2$. Calc.: C, 58.11; H, 3.39; N, 3.39%. IR: ν(CO), 1980w, 1930s, 1910s, 1882s, 1824s, 1800s, cm^{-1}. ^{31}P NMR: δ 84.37.

3.5. Synthesis of $(CO)_3Fe(\mu\text{-}Ph_2Ppy)_2AgClO_4$ (11)

The addition of a dichloromethane (15 ml) solution of **1** (0.4 g, 0.6 mmol) to a stirred benzene solution (10 ml) of $AgClO_4$ (0.15 g, 0.72 mmol) soon resulted in a

Table 9
Fe–Hg distances of some known complexes

Complex	Fe–Hg (Å)	Reference
$Cl_2HgFe[CS_2C_2(CO_2Me)_2](CO)_2(PMe_2Ph)_2$	2.546	[20]
$Fe(CO)_4(HgClpy)_2$	2.553	[21]
$[Fe(CO)_4(HgCl)(HgCl_2)]^-$	2.516; 2.560	[22]
$Hg[Fe(CO)_2(NO)(PEt_3)]_2$	2.534	[23]
$Fe(CO)_4(HgBr)_2$	2.44; 2.59	[24]
$Fe(CO)_4(HgSCN)_2$	2.506	[25]
$(OC)_3(Me_3P)(Ph_2MeSi)FeHgBr$	2.515	[14]
$Hg[Fe\{Si(OMe)_3\}(CO)_3(dppm\text{-}P)]_2$	2.574; 2.576	[15]

yellowish-green precipitate. The solution was filtered and reduced in volume to 8 ml, and diethyl ether was added. By slow evaporation of the solvent, the product was obtained as yellow crystals (0.34 g) in 64.9% yield. Anal. Found: C, 50.64; H, 3.48; N, 2.85. $C_{37}H_{28}AgClFeN_2O_7P_2$. Calc.: C, 50.80; H, 3.21; N, 3.21%. IR: ν(CO), 1990m, 1930s. 1892s, cm^{-1}. ^{31}P NMR: δ 83.77. FD-MS: m/e (relative intensity, %), 774 (M^+-ClO_4, 12), 633 ($Ag(Ph_2Ppy)_2^+-1$, 42).

3.6. Synthesis of $(CO)_3Fe(\mu\text{-}Ph_2Ppy)_2SnCl_2$ (12)

A THF solution (25 ml) containing **1** (0.4 g, 0.6 mmol) and $SnCl_2$ (0.12 g, 0.6 mmol) was left stirring for 4 h. During this time, the color changed from yellow to orange. Concentration of the solution to 8 ml followed by dilution with diethyl ether afforded a yellow solid which was filtered off and recrystallized from dichloromethane–diethyl ether to give the product as yellow crystals, 0.29 g in 55.8% yield. Anal. Found: C, 51.08; H, 3.33; N, 2.88. $C_{37}H_{28}Cl_2FeN_2O_3P_2Sn$. Calc.: C, 51.87; H, 3.27; N, 3.27%. IR: ν(CO), 2030s, 1990s, 1980s, cm^{-1}. ^{31}P NMR: δ 82.38.

3.7. Synthesis of $(CO)_3Fe(\mu\text{-}Ph_2Ppy)_2 \cdot HgCl_2$ (13)

A solution of **1** (0.4 g, 0.6 mmol) in 15 ml of 1:2 (v:v) of butanone-2 and benzene was added to a solution of $HgCl_2$ (0.33 g, 0.12 mmol) in the same solvent. After stirring for 1 h, a pale yellow precipitate (0.62 g) in 85.5% yield was formed. This was filtered, washed with diethyl ether and dried in vacuo. Anal. Found: C, 37.10; H, 2.51; N, 2.17. $C_{37}H_{28}Cl_4FeHg_2N_2O_3P_2$. Calc.: C, 36.72; H, 2.31; N, 2.31%. IR: ν(CO), 2010w, 1990m, 1975s, cm^{-1}. ^{31}P NMR: δ 70.94 (s, ^2J(Hg–P) = 219 Hz). FD-MS: m/e (relative intensity, %). 903 (M^+-HgCl_3, 100). 666 ($Fe(Ph_2Ppy)_2(CO)_3^+$, 27), 319 ($Fe(Ph_2Ppy)^+$, 8).

3.8. Synthesis of $(CO)_3Fe(\mu\text{-}Ph_2Ppy)_2HgI_2$ (14)

To a solution of **1** (0.4 g, 0.6 mmol) in dichloromethane (15 ml) was added a red solid HgI_2 (0.27 g, 0.6 mmol). The solid soon dissolved to give a yellow solution which was then stirred for 4 h. Concentration of the initial reaction mixture to 5 ml followed by addition of diethyl ether (20 ml) produced a pale-yellow crystal in 90.7% yield. Recrystallization could be accomplished from dichloromethane–diethyl ether. Anal. Found: C, 39.52; H, 2.56; N, 2.24. $C_{37}H_{28}FeHgI_2N_2O_3P_2$. Calc.: C, 39.63; H, 2.50; N, 2.50%. IR: ν(CO), 2010w, 1965s, cm^{-1}. ^{31}P NMR: δ 68.79 (s, ^2J(Hg–P) = 190 Hz). FD-MS: m/e (relative intensity, %). 992 (M^+-I, 100), 849 ($HgI(Ph_2Ppy)_2^+$, 78), 666 ($Fe(CO)_3(Ph_2Ppy)_2^+$, 36).

3.9. X-ray data collection and structure refinement for 1 and 14

Suitable yellow crystals of **1** and **14** were obtained by slow evaporation of benzene–methanol and dichloromethane–diethyl ether solutions respectively. For both **1** and **14**, a crystal of approximate dimension $0.2 \times 0.2 \times 0.3$ mm^3 was mounted on a glass fiber. Intensity data were collected on an Enraf–Nonius CAD4 diffractometer using graphite monochromated Mo Kα radiation (λ = 0.71073 Å). The measurements were carried out in the range $2 \leqslant \theta \leqslant 23°$ by ω–2θ scan technique at room temperature (23 ± 1°C), in which the reflections with $I \geqslant 3\sigma(I)$ were considered to be observed and used in the succeeding refinement. Corrections for Lp factors and for the absorption by empirical formula were applied to the data.

The structures of **1** and **14** were solved by the direct method (MULTAN 82). For **1**, the position of the Fe atom was found from the E-map; for **14**, the positions of the Fe atom and Hg atom were found from the E-map. The coordinates of the non-hydrogen atoms were obtained through several difference Fourier syntheses. For the coordinates and anisotropic thermal parameters of the non-hydrogen atoms full matrix least squares refinements were carried out. The two pyridinic N atoms had been clearly identified in the structure of **1** (see list of atomic coordinates and Fig. 1), even if it is very difficult to distinguish a carbon atom from a nitrogen atom. Satisfactory final unweighted and weighted agreement factors were obtained. The highest peaks in the final difference Fourier map were of 0.79 and 0.71 e $Å^3$. All

Table 10
Crystallographic data for **1** and **14**

	1·1/2C_6H_6	**14**
Formula	$C_{40}H_{31}FeN_2O_3P_2$	$C_{37}H_{28}FeHgI_2N_2O_3P_2$
Fw	705.5	1120.8
Color	yellow	yellow
Space group	$P2_1c$	$P2_1n$
Crystal system	monoclinic	monoclinic
a (Å)	17.560(5)	13.829(2)
b (Å)	12.110(1)	14.175(2)
c (Å)	18.176(4)	19.514(3)
β (deg)	101.27(2)	120.27(1)
Z	4	4
d_{calcd} (g cm^{-3})	1.24	1.992
Crystal size (mm^3)	0.2×0.2×0.3	0.2×0.2×0.3
μ (cm^{-1})	5.19	62.46
Final R	0.077	0.032
Final Rw	0.067	0.035
No. of unique reflections	5752	5360
No. of observed reflections	2670	3279

calculations were performed on a PDP11'44 computer with SDP-PLUS. Crystallographic data are summarized in Table 10.

3.10. Determination of electron-absorption spectra

The electron-absorption spectra were measured in a N_2 atmosphere with dichloromethane solvent or the dichloromethane solution of **1** as standard. The concentrations were $(2–5) \times 10^{-5}$ mol/dm^{-3}. Table 2 gives the results.

4. Supplementary material available

Tables giving fractional coordinates, thermal parameters, bond distances and angles for **1** and **14** (8 pages) are available. Ordering information is given on any current masthead page.

Acknowledgments

We wish to thank the National Science Foundation and Elemento-Organic Chemistry Laboratory, Nankai University for financial support.

References

[1] (a) M.M. Olmstead, C.H. Lindsay, L.S. Benner and A.L. Balch, *J. Organomet.Chem. 179* (1979) 293; (b) J.P. Farr, M.M. Olmstead and A.L. Balch, *J. Am. Chem. Soc., 102* (1980) 6654; (c) A. Maisonnat, J.P. Farr and A.L. Balch, *Inorg. Chim. Acta, 53* (1981) L217; (d) J.P. Farr, M.M. Olmstead, C.H. Hunt and A.L. Balch, *Inorg. Chem., 20* (1981) 1182; (e) M.M. Olmstead, A. Maisonnat, J.P. Farr and A.L. Balch, *Inorg. Chem., 20* (1981) 4060; (f) A. Maisonnat, J.P. Farr, M.M. Olmstead, C.T. Hunt and A.L. Balch, *Inorg. Chem., 21* (1982) 3961; (g) J.P. Farr, M.M. Olmstead, N.M. Rutherford, F.E. Wood and A.L. Balch, *Organometallics, 2* (1983) 1758; (h) J.P. Farr, M.M. Olmstead, F.E. Wood and A.L. Balch, *J. Am. Chem. Soc., 105* (1983) 792; (i) J.P. Farr, M.M. Olmstead and A.L. Balch, *Inorg. Chem., 22* (1983) 1229; (j) J.P. Farr, F.E. Wood and A.L. Balch, *Inorg. Chem., 22* (1983) 3387; (k) Z.Z. Zhang and H.K. Wang, *J. Organomet. Chem., 314* (1986) 357; (l) Z.Z. Zhang and H.K. Wang, *Gaodeng Xuexiao Huaxue Xuebao, 11* (1990) 255; (m) Z.Z. Zhang, H.P. Xi, W.J. Zhao, K.Y. Jiang, R.J. Wang, H.G. Wang and Y. Wu, *J. Organomet. Chem., 454* (1993) 221; (n) A.L. Balch, *Prog. Inorg. Chem., 41* (1994) 238; (o) C.G. Arena, G. Bruno, G. DeMunno, E. Rotondo, D. Drommi and F. Faraone, *Inorg. Chem., 32* (1993) 1601; (p) D. Drommi, C.G. Arena, F. Nicolò, G. Bruno and F. Faraone, *J. Organomet. Chem., 485* (1995) 115.

[2] (a) G. Bruno, S. LoSchiavo, E. Rotondo, C.G. Arena and F. Faraone, *Organometallics, 8* (1989) 886; (b) E. Rotondo, S. LoSchiavo, G. Bruno, C.G. Arena, R. Gobetto and F. Faraone, *Inorg. Chem., 28* (1989) 2944; (c) S. LoSchiavo, F. Faraone, M. Larfrarchi and A. Tiripicchio, *J. Organomet. Chem., 387* (1990) 357; (d) C.G. Arena, E. Rotondo and F. Faraone, *Organometallics, 10* (1991) 3877; (e) S. LoSchiavo, F. Rotondo, G. Bruno and F. Faraone, *Organometallics, 10* (1991) 1613; (f) E. Rotondo, G. Bruno, F. Nicolò, S. LoSchiavo and P. Piraino, *Inorg. Chem., 30* (1991) 1195; (g) G. Reinhard, B. Hirle, U. Schubert, M. Knorr, P. Braunstein, A. Decian and J. Fischer, *Inorg. Chem., 32* (1993) 1656.

[3] (a) D.F. Shriver, *Acc. Chem. Res., 3* (1970) 231; (b) D.F. Shriver, *J. Organomet. Chem., 94* (1975) 259; (c) J.M. Burlitch, in G. Wilkinson, F.G.A. Stone and E.W. Abel (eds.), *Comprehensive Organometallic Chemistry*, Vol. 6, Pergamon, New York, 1983, p. 983.

[4] H. Hock and H. Stuhlmann, *Chem. Ber. b, 61* (1928) 2097.

[5] D.J. Cook, J.L. Dawes and R.D.W. Kemmitt, *J. Chem. Soc.*, (1967) 1547.

[6] F.W.B. Einstein, R.K. Pomeroy, P. Rushman and A.C. Willis, *J. Chem. Soc. Chem. Commun.*, (1983) 854.

[7] F.W.B. Einstein, R.K. Pomeroy, P. Rushman and A.C. Willis, *Organometallics, 3* (1985) 250.

[8] J.A. Shipley, R.J. Batchelor, F.W.B. Einstein and R.K. Pomeroy, *Organometallics, 10* (1991) 3620.

[9] F.W.B. Einstein, M.C. Jennings, R. Krontz, R.K. Pomeroy, P. Rushman and A.C. Willis, *Inorg. Chem., 26* (1987) 1341.

[10] D.A. Roberts, W.C. Mercer, G.L. Geoffroy and C.G. Pierpont, *Inorg. Chem., 25* (1986) 1439.

[11] H. Nakatsuji, M. Hada and A. Kawashima, *Inorg. Chem., 31* (1992) 1740.

[12] J.R. Sowa, J.V. Zanotti, G. Fachin and R.J. Angelici, *J. Am. Chem. Soc., 113* (1991) 9185.

[13] (a) D.M. Adams, D.J. Cook and R.D.W. Kemmitt, *J. Chem. Soc.*, (1968) 1067; (b) P. Demerseman, G. Bouquet and M. Bigoryne, *J. Organomet. Chem., 35* (1972) 341.

[14] G. Reinhard, B. Hirle and U. Schubert, *J. Organomet. Chem., 427* (1992) 173.

[15] P. Braunstein, M. Knorr, A. Tiripicchio and M.T. Camellini, *Inorg. Chem., 31* (1992) 3685.

[16] C.K. Jørgensen, *Prog. Inorg. Chem., 4* (1962) 73.

[17] R. Krishnamurthy and W.B.J. Schaop, *J. Chem. Educ., 46* (1969) 799.

[18] Y.Q. Zhou, *Biophys. Chem., 42* (1992) 201.

[19] (a) A.B.P. Lever, in *Inorganic Electronic Spectroscopy*, Elsevier, Amsterdam, 2nd edn., (1984); (b) G.J. Ferraudi, in *Elements of Inorganic Photo-Chemistry*, Wiley–Interscience, New York, 1988.

[20] H. LeBozec, P.H. Dixneuf and R.D. Admas, *Organometallics, 3* (1984) 1919.

[21] R.W. Baker, *J. Chem. Soc. Chem. Commun.*, (1970) 573.

[22] P.D. Botherton, *J. Chem. Soc. Dalton Trans.*, (1976) 870.

[23] F.S. Stephens, *J. Chem. Soc. Dalton Trans.*, (1972) 2257.

[24] H.W. Barrd and F.D. Laerence, *J. Organomet. Chem., 7* (1967) 503.

[25] A.E. Manro, *Polyhedron, 6* (1987) 1273.

[26] D.P. Tate, W.R. Knipple and J.M. Angl, *Inorg. Chem., 1* (1962) 433.